This article has been accepted for inclusion in a future issue of this journal. Content is final as presented, with the exception of pagination.

Fast Current-Only Based Fault Detection Method in Transmission Line

Mohammad Amin Jarrahi, Haidar Samet, *Member, IEEE*, and Teymoor Ghanbari, *Member, IEEE*

***Abstract*—When a fault occurs in transmission lines, first, it is detected, then classified, and finally, located by a distance protection. Having a fast fault detection approach helps saving the required time for the whole protection procedure. In this paper, a novel method for fault detection of transmission lines based on the summation of squared three-phase currents (SSC) and a moving average technique is proposed. The SSC is constant during a normal condition of the network, while it has considerable variation under a fault condition. Using a moving average concept, a criterion is defined, by which fault occurrence can be detected. The proposed fault detection method is evaluated in four different systems: a typical 5-bus system, a typical double-circuit transmission line, WSCC 9-bus system, and a laboratory small-scaled system. The results confirm a high degree of accuracy and speed of the proposed approach. Moreover, the performance of the method is compared with some other similar methods from different aspects.**

***Index Terms*—Distance relay, fault detection, moving average, transmission line (TL).**

I. Introduction

A. Motivation and Literature Review

TRANSMISSION lines (TLs) are vital channels of conventional power systems because power transmission through them is the sole path for power delivery from generation units to load centers. These lines pass through impassable areas with a high possibility of fault occurrence because of experiencing severe environmental conditions. Therefore, protection of TLs is one of the critical topics for operators of power systems. There are several approaches for protection of TLs, among which distance protection is more efficient. In general, a distance protection has three series stages including detection, classification, and location [1]. Here, the aim is to promote the performance of the detection stage of this protection.

In addition to fault detection, the required information for the next steps is gathered in the fault detection stage. Fault type is determined in a fault classification stage, and the distance of the fault from the protection relay is estimated in a fault location stage. In these consecutive stages, classification and location steps will be performed when the fault is detected by the first stage. Therefore, having a fast protection scheme depends on the speed of the detection approach. Fault classification step should also be accomplished precisely because its information is required for the other steps [2]–[5].

Up to now, many techniques have been proposed for fault detection in TLs [6]–[11]. These techniques can be classified into several groups as follows:

A) signal processing-based techniques [12], [13];
B) phasor-based techniques [14];
C) artificial intelligence (AI)-based techniques [15]–[17];
D) traveling wave-based techniques [18], [19];
E) miscellaneous techniques [20]–[22].

Fig. 1 shows different approaches of the mentioned groups.

There are some indices that can be utilized to compare these techniques including fault detection speed, accuracy, computational burden, flexibility for different fault scenarios and systems, input signals, and sampling rate. Table I represents a qualitative comparison between the groups and proposed method. Group A contains signal processing-based techniques such as wavelet transform-based methods [12] and Fourier transform-based ones [13]. Group B includes phasor-based techniques such as voltage rms-based methods, current rms-based methods as well as voltage and current rms-based ones [14]. Group C comprises techniques based on AI such as artificial neural network [15], support vector machine [16], and decision tree [17]. Group D involves traveling wave-based techniques [18], [19]. Other techniques that are not included in the previously mentioned groups are gathered in Group E, entitled miscellaneous group. This group contains techniques such as correlation-based methods [20], fuzzy logic-based methods [21], sequential component-based ones [22], etc.

The main conclusions of the presented comparison in Table I can be addressed as follows.

1) *Group A:* Input signals of this group are usually three-phase currents, preferred over the methods that require both voltage and current signals. Generally, delay time of this group is about 5 ms, which is high enough. High computational burden is the main drawback of this group. Also, settings of these techniques should be readjusted to work properly for different systems. The accuracy of this group highly depends on the tuning of the methods for under-study systems. In comparison with the other methods, they have lower accuracy in general. Moreover, they need a high sampling frequency to have acceptable performance.

Manuscript received October 5, 2017; revised January 14, 2018; accepted March 4, 2018. *(Corresponding author: Haidar Samet.)*

M. A. Jarrahi and H. Samet are with the School of Electrical and Computer Engineering, Shiraz University, Shiraz 71348-51154, Iran (e-mail: ma.jarrahi@shirazu.ac.ir; samet@shirazu.ac.ir).

T. Ghanbari is with the School of Advanced Technologies, Shiraz University, Shiraz 71946-84636, Iran (e-mail: ghanbarih@shirazu.ac.ir).

Digital Object Identifier 10.1109/JSYST.2018.2822549

1937-9234 © 2018 IEEE. Personal use is permitted, but republication/redistribution requires IEEE permission.
See http://www.ieee.org/publications_standards/publications/rights/index.html for more information.

This article has been accepted for inclusion in a future issue of this journal. Content is final as presented, with the exception of pagination.

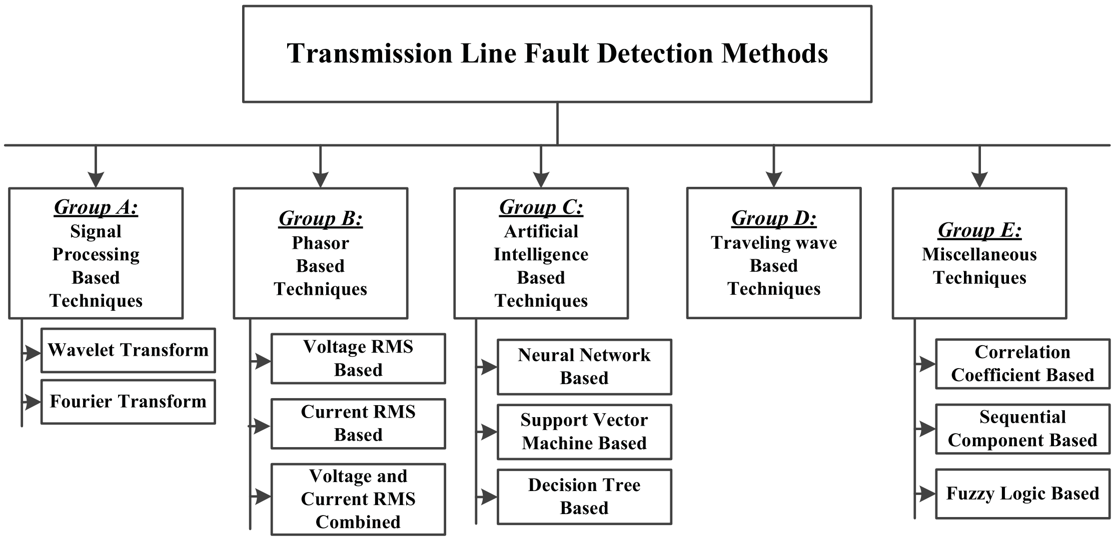

Fig. 1. Techniques utilized for TL fault detection in different groups.

TABLE I
QUALITATIVE COMPARISON BETWEEN DIFFERENT GROUPS AND PROPOSED METHOD

Method	*Input signals*	*Speed*	*Accuracy*	*Computational burden*	*Need of readjusting*	*Sampling rate*
Group A	Current	High	High	High	Yes	High
Group B	Current and voltage	Low	Low	High	Yes	High
Group C	Current and voltage	High	High	Very High	No	-
Group D	Current and voltage	High	High	High	Yes	Very High
Group E	Current and voltage	Medium	High	Low	Yes	Low
Proposed Method	Current	Very High	Very High	Very Low	No	Low

2) *Group B:* All features of this group depend on the selected phasor estimation method. If the method is not selected properly, their performance degrades dramatically. Considering the presented comparison, this group is not a good option for the detection.
3) *Group C:* Although the AI-based approaches are able to detect faults efficiently, considerable amount of training effort for having a good performance is one of the main disadvantages of these methods. For the power systems that have a wide variation of operating conditions, this problem is more considerable.
4) *Group D:* The main requirement of techniques in this group is high sampling rate measurement devices. Although the methods of this group are fast and accurate, utilizing the high sampling rate measurement devices affects the advantages, considerably.
5) *Group E:* Low computational burden and no need of a high sampling frequency rate are the main merits of this group. However, some limitations in terms of increasing the accuracy and speed exist. Moreover, fault location, fault resistance, and fault inception angle have considerable impacts on their performance.

Some of the common situations in which the already presented methods have some shortcomings and may have wrong operation are complexity in modern power systems, faults with high resistances, power swing situations, heavy load switching into TLs, presence of noise in measured waveforms, effect of mutual coupling in double-circuit TLs, permanent change in effective factors associated with the fault in TL, i.e., fault inception angle, fault location, different load angles, etc. These conditions may affect voltage and current waveforms at initial moments after fault occurrence, which may lead to malfunctioning of the protection algorithms. As a result, finding a reliable, accurate, and fast fault detection technique is an open problem in distance protection of TL, yet.

B. Aim and Contribution

In this paper, a novel protection scheme is proposed to detect faults in TLs. The method is based on three-phase currents and a moving average concept. Procedure of the proposed method starts with the calculation of the summation of squared three-phase currents (SSC). In the next stage, a 10 ms moving window with 1 ms sliding time step as the moving average is applied to the SSC. The SSC is constant during normal operation of the system, but it experiences considerable variation in fault situation. Considering these changes, a novel criterion based on the moving average technique is defined to identify faults. The proposed method is evaluated using four different systems under various conditions. The results confirm that faults can be detected in less than 1.7 ms after fault occurrence with a desirable accuracy.

Considering the discussion in Table I, the main contributions of the proposed method can be summarized as follows.

1) processing only one signal, which is a combination of three-phase current signals;
2) low computational burden and cost efficient as there is no need of a voltage transformer;
3) no need of readjusting for different network structures;
4) taking into account heavy load connection in the evaluation of the method;
5) having relatively high accuracy and speed.

C. Paper Organization

In the rest of the paper, Section II presents a detailed explanation about the proposed fault detection method. In Section III, the utilized systems for evaluation of the method are introduced. Section IV explains the performance of the proposed method under different conditions. Section V describes the comparison of the method with some other similar techniques. Finally, conclusions are given in Section VI.

II. Proposed Fault Detection Method

In the presented method, measured instantaneous three-phase currents are the input signals. Having instantaneous currents from one end of the TL, SSC is defined as follows:

$$\mathrm{SSC} = i_A^2\,(t) + i_B^2\,(t) + i_C^2\,(t) \tag{1}$$

where i_A, i_B, and i_C are three-phase currents measured at relay location. This signal is constant during normal operation of power systems, but it has abrupt change after a fault occurrence.

In order to confirm this claim, first it is assumed that the measured three-phase currents of the TL are as follows:

$$\begin{aligned} i_A\,(t) &= I_{\mathrm{mA}} \cos\left(\omega t + \varphi_A\right) \\ i_B\,(t) &= I_{\mathrm{mB}} \cos\left(\omega t + \varphi_B - 120^\circ\right) \\ i_C\,(t) &= I_{\mathrm{mC}} \cos\left(\omega t + \varphi_C + 120^\circ\right) \end{aligned} \tag{2}$$

where I_{mA}, I_{mB}, and I_{mC} are the maximum values of three-phase currents and φ_A, φ_B, and φ_C are the relevant phase angles. Two situations are considered for this assessment, which are discussed as follows.

A. Normal Condition

Transmission networks can be assumed balanced and symmetric in normal operation [23]. Under this condition, the maximum values of three-phase currents and phase angles are almost equal, as presented in (3). The phase angles are also assumed as follows for more simplification

$$\begin{aligned} I_{\mathrm{mA}} &= I_{\mathrm{mB}} = I_{\mathrm{mC}} = I_m \\ \varphi_A &= \varphi_B = \varphi_C = \varphi \\ \omega t + \varphi &= \theta. \end{aligned} \tag{3}$$

Therefore, SSC can be calculated as follows:

$$\mathrm{SSC}_{\mathrm{normal}} = I_m^2 \left[\frac{3}{2} + \frac{\cos\left(2\theta\right)}{2} + \frac{\cos\left(2\theta - 240^\circ\right)}{2} + \frac{\cos\left(2\theta + 240^\circ\right)}{2}\right]. \tag{4}$$

In (4), the resultant of three sinusoidal terms is zero and therefore

$$\mathrm{SSC}_{\mathrm{normal}} = \frac{3}{2} I_m^2. \tag{5}$$

From (5), it is confirmed that the value of SSC is constant during normal operation of the system.

B. Fault Condition of the System

Fault current signals in TLs generally have a dc offset component, which can be expressed as decaying exponential functions [23]. Generally, fault current signals for each phase can be represented as follows:

$$i\,(t) = I_0 e^{-\frac{t}{\tau}} + I_m' \cos\left(\omega t + \varphi'\right). \tag{6}$$

In (6), I_0 and τ are magnitude and time constant of the decaying dc offset, respectively. Also, it is obvious that the maximum value of current I_m' and phase angle φ' is different under fault and normal conditions.

Here, a three-phase symmetrical fault is considered as a typical fault for discussion about the variation of SSC signals considering a fault current signal presented in (6). However, the study can be developed for any other fault types by the same approach. Also, it is assumed that the decaying dc component appears in all the phases. Moreover, the maximum value, phase angle, dc offset magnitude, and time constant for all the phases are considered identical

$$\begin{aligned} \mathrm{SSC}_{\mathrm{fault}} = {} & I_m'^2 \cos^2\left(\theta'\right) + I_m'^2 \cos^2\left(\theta' - 120^\circ\right) \\ & + I_m'^2 \cos^2\left(\theta' + 120^\circ\right) + 3 I_0^2 e^{-\frac{2t}{\tau}} + 2 I_0 I_m' e^{-\frac{t}{\tau}} \\ & \left[\cos\left(\theta'\right) + \cos\left(\theta' - 120^\circ\right) + \cos\left(\theta' + 120^\circ\right)\right]. \end{aligned} \tag{7}$$

Here, SSC can be written as

$$\mathrm{SSC}_{\mathrm{fault}} = \frac{3}{2} I_m'^2 + 3 I_0^2 e^{-\frac{2t}{\tau}}. \tag{8}$$

Equation (8) shows that SSC changes over time under the fault condition. Moreover, the constant term in this equation is different from the corresponding term under the normal condition.

To make a suitable criterion for detection of the change in SSC, a moving average is applied to this signal. The moving average for a given discrete signal like $x_n(t)$ in a window with length T_0 is defined by [24]

$$\mathrm{MA}_n = \frac{1}{T_0} \sum_{n=t-T_0}^{t} x_n\,(t) \tag{9}$$

in which MA_n denotes the moving average of signal $x(t)$ in the nth window. In the proposed method, moving average is applied to the SSC signal with the window length of 10 ms and the time

This article has been accepted for inclusion in a future issue of this journal. Content is final as presented, with the exception of pagination.

step of 1 ms. The proposed fault detection criterion (FDC) is defined as the ratio of each window's average for the SSC signal to its last window average as follows:

$$\mathrm{FDC}_n = \frac{\mathrm{MA}_n}{\mathrm{MA}_{n-1}}. \tag{10}$$

Value of FDC is very close to one under the normal condition. But, it has some deviations from one under the fault condition. Since the value of the SSC signal is constant in the normal operation, mean values of two typical consecutive windows are equal. Consequently, the ratio of them, named FDC, is very close to one. The minor deviations of FDC from unity under this condition refer to the presence of different noises in the signals. By comparing this value with a predefined threshold, the fault can be detectable. If FDC exceeds a predefined threshold, it is detected as a fault.

The following equation defines this logic for fault detection in TLs. In this equation, *nf* in FDC_{nf} determines the window in which the fault is detected and parameter TH denotes the threshold

$$\mathrm{FDC}_{nf} > \mathrm{TH} \rightarrow \mathrm{Fault}. \tag{11}$$

Value of the threshold is considered 1.1 based on plenty of simulations and experiments. This threshold is constant for different systems because the proposed FDC is a self-comparing index and it is not related to the magnitude of the SSC signal. It should be mentioned that the selection of the threshold for fault detection techniques is a challenging task, which can be accomplished by different approaches. In this paper, a straightforward method named Otsu thresholding method is considered to set the threshold. More information about this method can be found in [25] and [26].

Flowchart of the proposed method is shown in Fig. 2(a). Fig. 2(b) and (c) shows SSC signal and corresponding FDC for a typical single line to ground fault. Fig. 2(b) demonstrates the SSC signal with the relevant processing windows. Window $n + 4$ is the first window, which includes samples relevant to the fault. In Fig. 2(c), the corresponding FDC is presented. As shown, the fault is detected in window $n + 6$.

Heavy load switching is generally similar to the fault condition in TLs. A considerable number of fault detection algorithms may have wrong operation under this condition. One of the main advantages of the proposed method is discrimination between heavy load switching and fault conditions with a desirable accuracy. Fig. 3 shows a comparative graph of the SSC signal for fault conditions [including single line to ground (LG), double lines to ground (LLG), line-to-line (LL), and three phases (3L)] and heavy load switching conditions (including capacitor bank switching, reactor switching, and resistive and resistive–inductive loads switching). As observed, the variation of SSC signals is different under normal and faulty conditions. In the proposed method, this difference is utilized to separate heavy loads switching from faults.

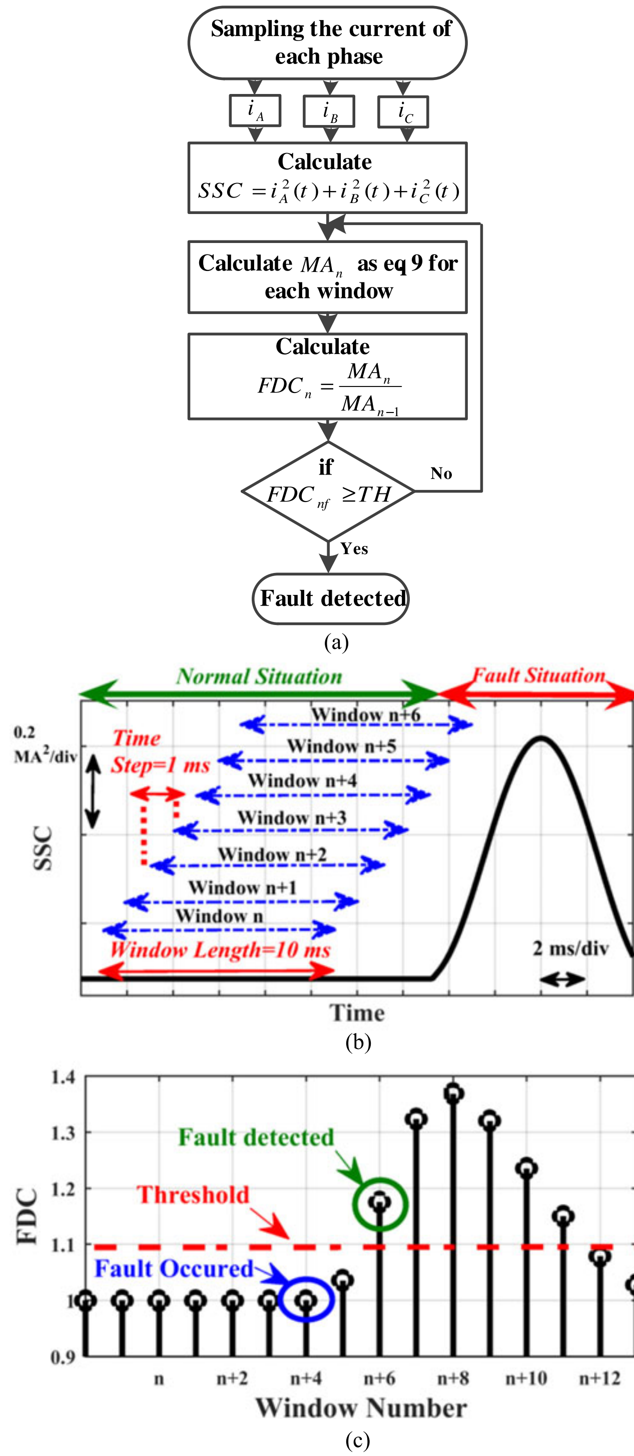

Fig. 2. (a) Flowchart of the proposed method. (b) SSC signal for a typical LG fault and the moving windows. (c) Corresponding FDC of the fault.

III. Test Case Systems

In this section, four different power systems including a typical 5-bus system, a typical double-circuit TL, a WSCC 9 bus system, and a laboratory small-scaled system for the evaluation of the proposed method are introduced. In the following, specifications of the systems are presented in more detail.

This article has been accepted for inclusion in a future issue of this journal. Content is final as presented, with the exception of pagination.

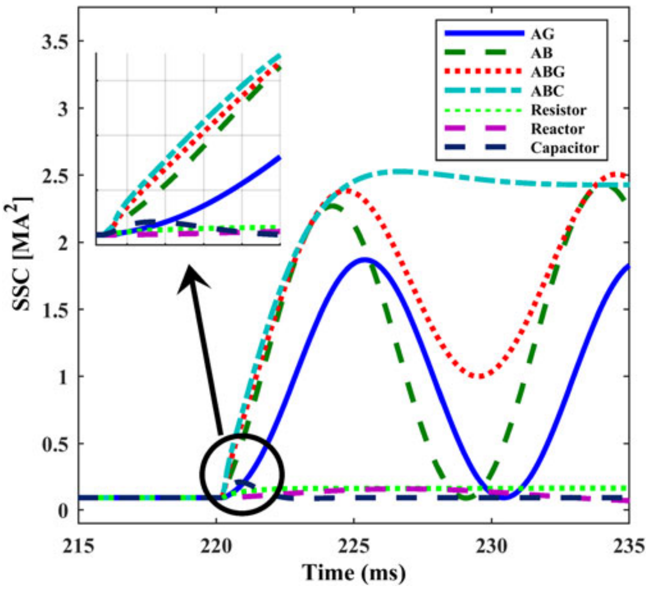

Fig. 3. SSC signal for different faults and heavy loads switching conditions.

A. First System: A Typical 5 Buses System

This system is a five-buses network, which has been utilized in [8] and [27]. It is simulated in MATLAB/SIMULINK software, and its single line diagram is shown in Fig. 4(a). This system has two generators, four transformers, and two loads connected to buses 4 and 5. The detailed parameters of the system are as follows.

1) *Generators:* rated LL voltage is 20 kV, three-phase short-circuit power is 1000 MVA, frequency is 50 Hz, and *X/R* ratio is 10. Voltage phase angle of generators 1 and 2 is 0° and –10°, respectively.
2) *Transformers:* rated power is 600 MVA, voltage ratio is 20/230 kV with delta-star-grounded connection, with $0.002 + j0.1$ p.u. impedance.
3) *Lines:* All line impedances are $0.02 + j0.15$ Ω/km with negligible capacitance. Lines 1–2, 2–3, 3–4, 4–1, and 5–2 are 50, 35, 60, 20, and 25 km, respectively.
4) *Loads:* rated LL voltage is 20 kV and the frequency is 50 Hz. The active and reactive powers of load 1 are 500 MW and 100 MVAr, respectively. The active and reactive powers of load 2 are 100 MW and 50 MVAr, respectively.

Simulation time step is set as 100 μs, which makes 200 samples per cycle in a 50 Hz system (sampling frequency is 10 kHz). Line between bus 1 and bus 2 is selected for the investigation. Current signals are captured from one end of the line. More than 350 different test cases in this system are considered for evaluating the proposed method.

B. Second System: A Typical Double-Circuit TL

This double-circuit TL is a common system, which has been utilized for evaluating the effect of mutual coupling between the circuits [28]. This system consists of a double-circuit TL with 220 kV and 100 km, connected to two sources at both ends. Short-circuit capacity of the sources is 1.25 GVA and their *X/R* is 10. The double-circuit TL is simulated in MATLAB/SIMULINK software using the distributed parameter line model. The required data at the beginning of the TL are captured with the sampling frequency of 10 kHz. More than 100 different test cases for each circuit (more than 200 cases for the system) are considered for the evaluation of the proposed method. The detailed parameters of the TL and single line diagram of the system are presented in Table II and Fig. 4(b).

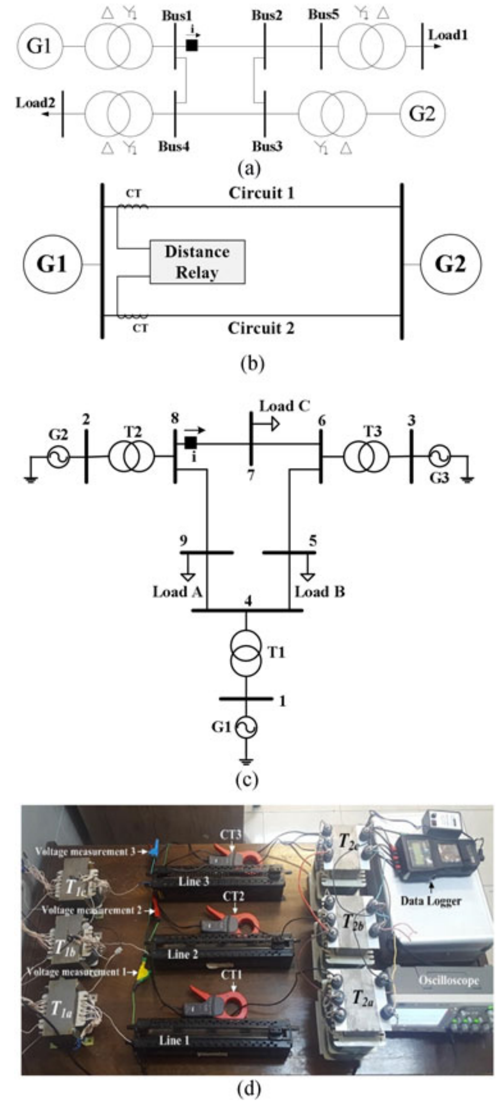

Fig. 4. Employed systems for the evaluation. (a) A typical 5 buses system [8], [27]. (b) A typical double-circuit based system [28]. (c) WSCC 9 buses system [29]. (d) Laboratory small-scaled system.

C. Third System: WSCC 9 Bus System

This system is a simplified version of Western System Coordinating Council (WSCC) as an equivalent system, which is simulated in PSCAD/EMTDC. Single line diagram of a WSCC 9 buses system is shown in Fig. 4(c). This test system consists of nine buses, three generators, three transformers, six TLs, and three loads, in which the nominal frequency is 60 Hz.

Primary voltages of the transformers are 18 kV and their secondary voltages are 230 kV. Detailed parameters of this system

This article has been accepted for inclusion in a future issue of this journal. Content is final as presented, with the exception of pagination.

TABLE II
PARAMETERS OF THE DOUBLE-CIRCUIT TL [28]

PARAMETER	*VALUE*
POSITIVE SEQUENCE RESISTANCE R1, Ω/KM	0.01809
ZERO SEQUENCE RESISTANCE R0, Ω/KM	0.2188
ZERO SEQUENCE MUTUAL RESISTANCE R0M, Ω/KM	0.20052
POSITIVE SEQUENCE INDUCTANCE L1, H/KM	0.00092974
ZERO SEQUENCE INDUCTANCE L0, H/KM	0.0032829
ZERO SEQUENCE MUTUAL INDUCTANCE L0M,H/KM	0.0020802
POSITIVE SEQUENCE CAPACITANCE C1, F/KM	1.2571×10^{-8}
ZERO SEQUENCE CAPACITANCE C0, F/KM	7.8555×10^{-9}
ZERO SEQUENCE MUTUAL CAPACITANCE C0M,F/KM	-2.0444×10^{-9}

have been reported in [29]. In this case study, the TL between bus 7 and bus 8 is considered. About 100 different test cases are simulated. Sampling frequency of currents and voltages signals is considered 10 kHz.

D. Fourth System: Laboratory Small-Scale System

In order to validate the performance of the proposed method in practice, a simple power system was implemented as a low-scale laboratory test bench. The system currents and voltages data were gathered using a data logger with the sampling frequency of 7.8 kHz. Fig. 4(d) shows the implemented system in more detail. More than 60 test cases with different conditions of the fault are gathered for evaluating the proposed method.

IV. SIMULATION AND RESULTS

Different scenarios are considered for the systems. These conditions are different types of faults, faults with high resistance, faults near boundaries, heavy load switching, presence of noise in signals, power swing situation, mutual coupling effect in double-circuit TLs, intercircuit faults in double-circuit TLs, faults in a series-compensated TL, CT saturation effect, and experimental data. In the following, the capability of the method is evaluated in these situations.

A. Various Fault Types

To simulate this condition, a fault is applied at the middle of the line between bus 1 and bus 2 in the first system at 220 ms. In this case, it is supposed that the fault and ground have very small resistances. Fig. 5(a), (b), (c), and (d) are the SSC signal and their FDC for LG fault, LL fault, LLG fault, and 3L fault, respectively. In these figures, the blue and green circles indicate the windows at which the samples relevant to the fault are entered and the fault is detected, respectively. Delay of the proposed method is determined by subtraction of the green circle numbers from the blue ones. For example, in Fig. 5(b), the fault is applied at window number 211 and it is detected at window number 212 with a delay time of 1 ms.

B. Faults With High Resistances

Detection of high resistance faults is a challenge for most of the algorithms [30]. There is a certain value of the high resistance fault, at which the algorithms may not be able to detect correctly.

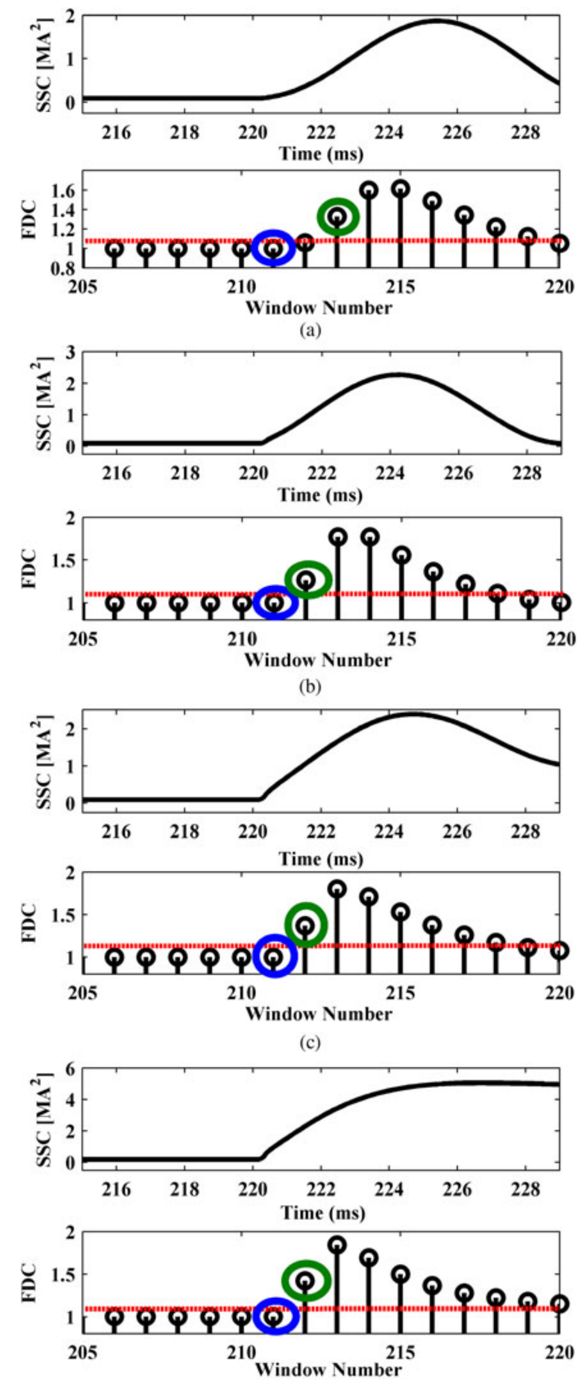

Fig. 5. SSC signals and their FDCs for different fault types in the first system with negligible fault resistance. (a) LG fault. (b) LL fault. (c) LLG. (d) 3L fault.

For evaluation of the proposed method, in this case, a three-phase fault with 300 Ω is applied at time 220 ms in the first system. As observed in Fig. 6, this case is detected after 1 ms. The proposed method is able to detect faults with the resistance about 300 Ω in the first system, 260 Ω in the second system, and 350 Ω in the third system.

C. Faults Near Boundaries

Faults near boundaries are one of the major challenges for the fault detection methods [31]. These fault types contain two

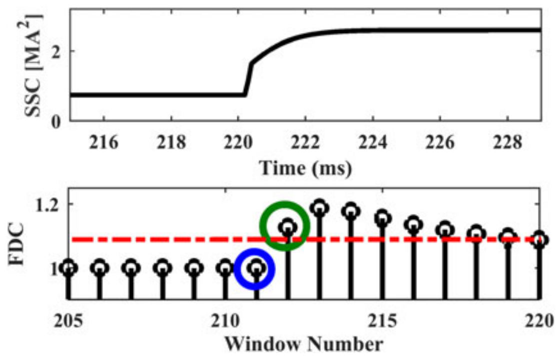

Fig. 6. SSC signal and its FDC for the LLL fault in the first system with the fault resistance of 300 Ω.

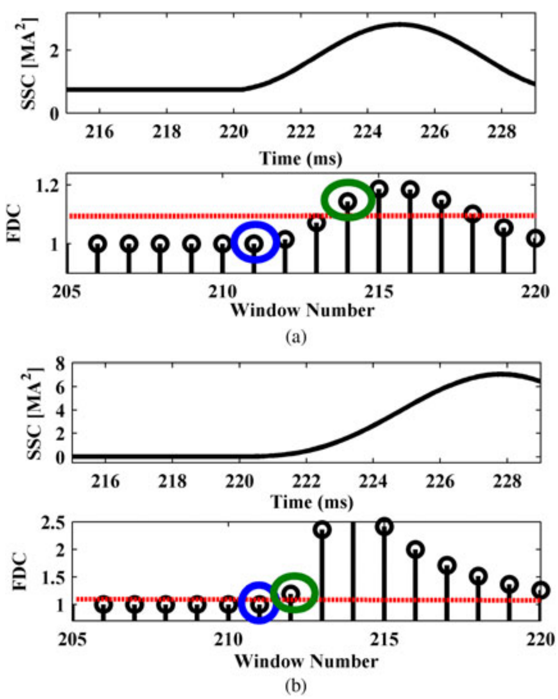

Fig. 7. SSC signals and their FDCs for faults near boundaries in the first system. (a) Far-end fault with the fault resistance of 320 Ω. (b) Close-in fault with negligible resistance.

conditions including far-end faults and close-in ones. Far-end faults are the faults that occur far from the relay location and close-in faults are faults that occur near the relay location.

In order to evaluate the proposed technique in case of far-end faults, different fault types at different locations (between 85% and 99% away from the relay location at bus 1 of the first system) are simulated. Also, to evaluate the performance of the method in case of close-in faults, various near faults at locations about 1–5% away from the relay location are considered. Fig. 7(a) shows the SSC and FDC for a typical LG fault occurring at 220 ms at location 95% of the mentioned line (47.5 km) as a far-end fault. Fault resistance is considered 320 Ω to simulate the worst case. It is observed that the fault is detected 3 ms after fault occurrence.

In Fig. 7(b), a close-in LG fault occurs at 220 ms at location 2.5% of the line (1.25 km). The proposed method can detect it

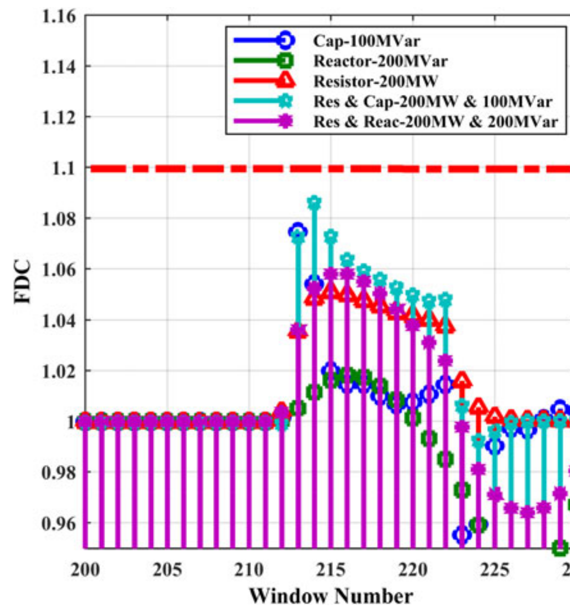

Fig. 8. FDC for different heavy load switching conditions in the first system.

after 1 ms. In this case, fault resistance is considered a small value to simulate the worst case.

D. Heavy Load Switching

One of the advantages of the proposed method is discrimination between faults and heavy load switching conditions with a desirable accuracy. When a heavy load is connected to the network, the TL current increases, significantly. This condition is very similar to fault occurrence in the TL, which results in wrong operation of the detection methods. Five different situations are considered in the first system to assess the performance of the proposed approach. Fig. 8 shows these situations that are relevant to switching of a resistive load with 200 MW, an inductive–resistive load with 200 MW and 200 MVAR, a resistive-capacitive load with 200 MW and 200 MVAR, a reactor with 200 MVAR, and a capacitor bank with 100 MVAR to the secondary side of the transformer connected to bus 5. As observed, FDC of the heavy load connections does not exceed the threshold and so the method does not have wrong operation. The results for second and third systems are similar to the results of the first system.

E. Presence of Noise in the Measured Signals

Generally, measured signals captured from real power systems contain noises [12]. Therefore, in order to simulate the noisy condition in the gathered data of real power systems, three white Gaussian noises with 20, 30, and 40 dB signal-to-noise ratios (SNRs) are added to the measured signals of the first system. Any SNR value of a signal is calculated by

$$\mathrm{SNR} = 10 \log \frac{P_s}{P_n}\,(\mathrm{dB}) \tag{12}$$

in which P_n is the power of the noise and P_s is the power (variance) of the signal. Fig. 9 displays the SSC signal for three

This article has been accepted for inclusion in a future issue of this journal. Content is final as presented, with the exception of pagination.

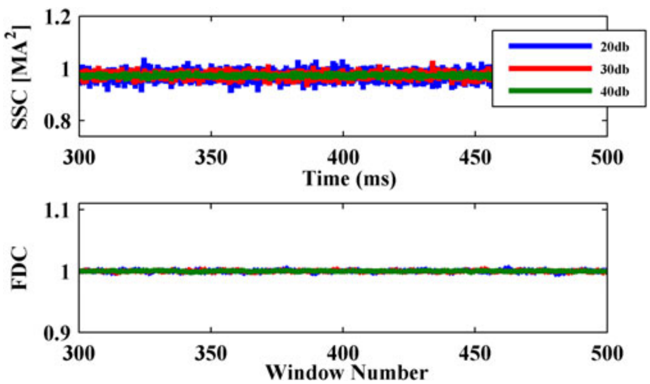

Fig. 9. SSC signals and their FDCs for different noisy conditions in the first system.

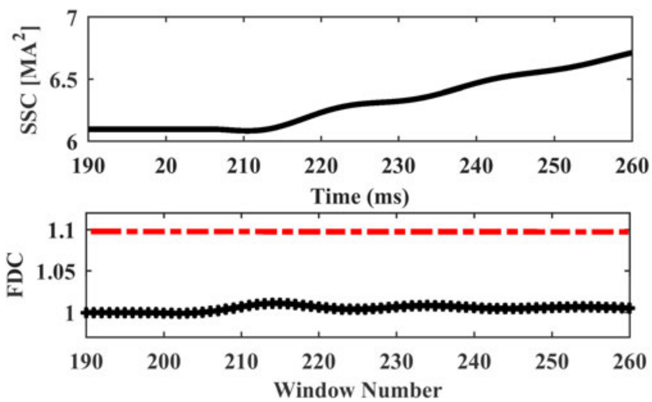

Fig. 10. SSC signal and its FDC for power swing situation in the first system.

different noisy conditions and the corresponding FDCs. The results confirm that the proposed method can preserve its performance under noisy conditions.

F. Power Swing Situation

In this case, the effect of power swing phenomena on the performance of the proposed scheme is studied. Power swings in electrical networks may occur because of system faults, line switching, generator outage, and disconnection of large loads. In these situations, electrical power has sudden variations, while the input mechanical power of generators remains constant. The injected energy by the rotors would increase the rotor angular velocity, which in turn leads to power swings. False operation of distance relays under the power swing condition is a common challenge. Therefore, the fault detection unit of distance relay should discriminate power swing phenomenon from the fault condition [32].

In the first system, assume that the voltage angle of G1 varies up to 45° with 1 Hz frequency at time 210 ms for emulation of power swing. Since dynamic of this variation is low, the proposed method does not have wrong operation under this condition, as shown in Fig. 10.

G. Double-Circuit TLs Challenges

Fault detection in double-circuit TLs is a challenging task because of the mutual coupling effect between both the circuits and incidence of intercircuit faults [33].

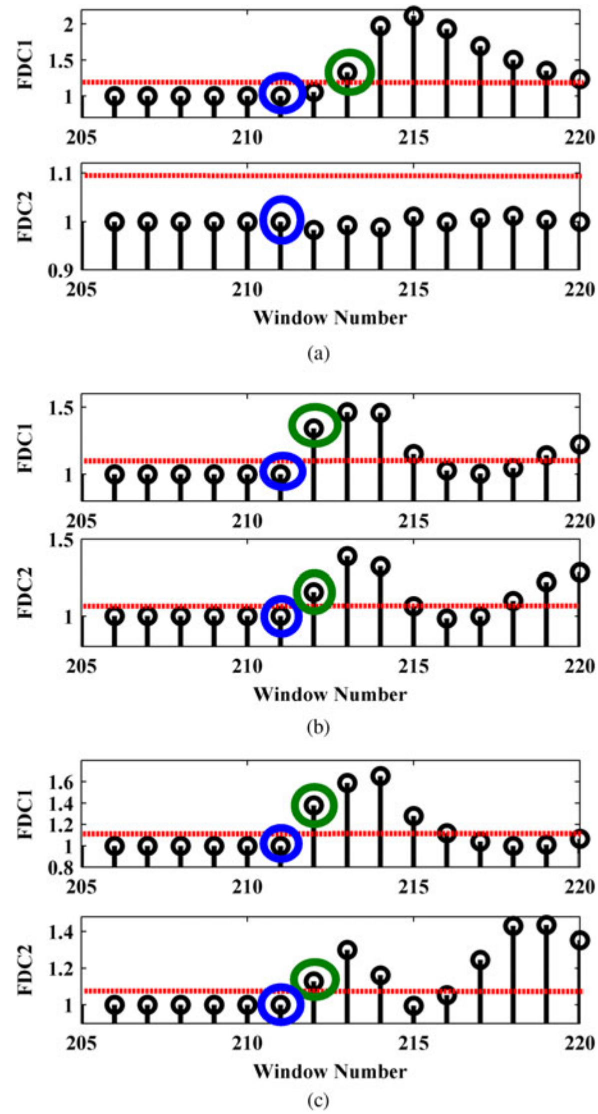

Fig. 11. FDC of each circuit in a double-circuit TL for different faults. (a) LG fault in circuit 1. (b) Intercircuit A1B2 fault. (c) Intercircuit A1B2G fault.

For simulating the effect of mutual coupling on the proposed method, an LG fault is applied to circuit 1 of the second system. Fig. 11(a) shows the corresponding FDC for each circuit in this situation, in which FDC1 and FDC2 are relevant to circuits 1 and 2, respectively. It is obvious that the proposed method can detect circuit 1 as a faulty circuit, straightforwardly.

Intercircuit faults are the faults that occur between two different phases of the circuits at the same location in double-circuit TLs. To evaluate the performance of the proposed method in these types of faults, two different conditions are considered including fault occurrence as A1B2 (phase A of circuit 1 and phase B of circuit 2) and fault occurrence as A1B2G (phase A of circuit 1 and phase B of circuit 2 are faulty phases with ground connection).

Fig. 11(b) and (c) shows the corresponding FDC for each circuit under the above-mentioned intercircuit faulty conditions. As seen, the proposed method detects both circuits as a faulty circuit under the mentioned faulty conditions, successfully.

This article has been accepted for inclusion in a future issue of this journal. Content is final as presented, with the exception of pagination.

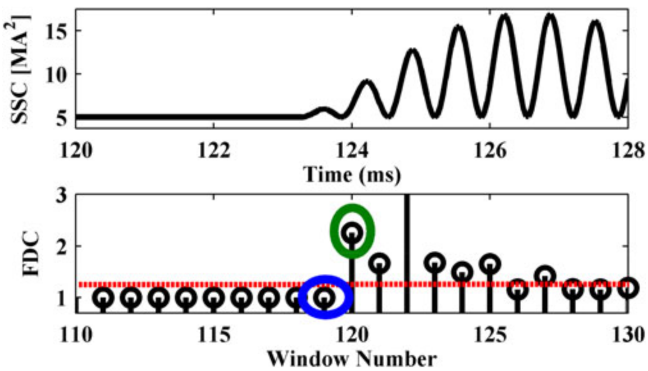

Fig. 12. SSC signal and its FDC for an LG fault in the third system with a series-compensated TL.

H. Faults in a Series-Compensated TL

Series compensation has been proven as a quite advantageous approach in long-distance power transmission. By reducing inductive reactance of TLs, the power transfer capacity, power losses, and the steady state as well as transient stability of the system can be improved. Despite all the mentioned benefits, these devices also produce some problems for the systems' protections. During a fault in a series-compensated TL, impedance characteristic of the network will be nonlinear and high-frequency noise will be generated. Consequently, significant distortions may appear in voltage and current waveforms, which may lead to false operation of the detection methods [34]. To simulate this condition, a series capacitor that provides 60% of compensation is located in the middle of the line between buses 7 and 8 in the third system. For the protection of the capacitor against overvoltage, a metal oxide varistor is utilized. For assessment of the method, plenty of simulations are carried out under this condition. Fig. 12 shows a typical result, in which an LG fault with 50 Ω is applied in the front of a series capacitor (fault location is 70% of the TL length). As observed, the fault is detected after 1 ms of fault occurrence.

I. CT Saturation Effect

Current transformers (CTs) may be saturated because of large amplitude of fault current and the presence of decaying dc offset. CT saturation causes severe distortion in the measured current waveform, which may cause wrong operation of fault detection algorithms with current as input signals [35]. In order to evaluate the effect of CT saturation on the performance of the proposed fault detection algorithm, some saturable CTs are used to measure the current of the TL shown in Fig. 4. The CTs are 1600 A/5 A, 25 VA and they saturate at 7.5 p.u. The capability of the proposed method was evaluated under this condition using many simulations. As a typical result, a 3L fault with 20 Ω resistance considering the CT saturation effect with the relevant SSC and FDC is shown in Fig. 13. It is obvious that the algorithm is able to detect the fault within 2 ms after fault inception. The test results confirm the capability of the suggested algorithm even for high dc offsets, which lead to CT saturation.

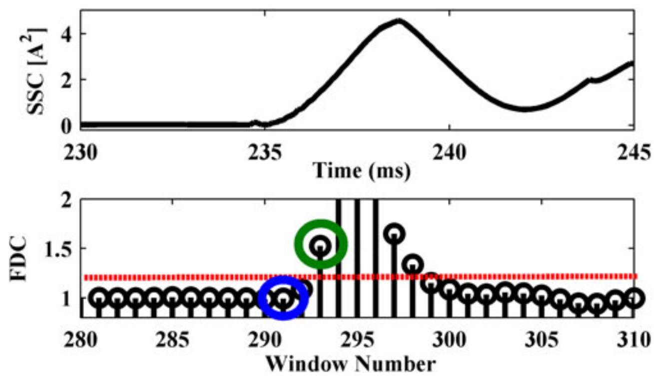

Fig. 13. SSC signal and its FDC for an LLL fault in the first system with CT saturation.

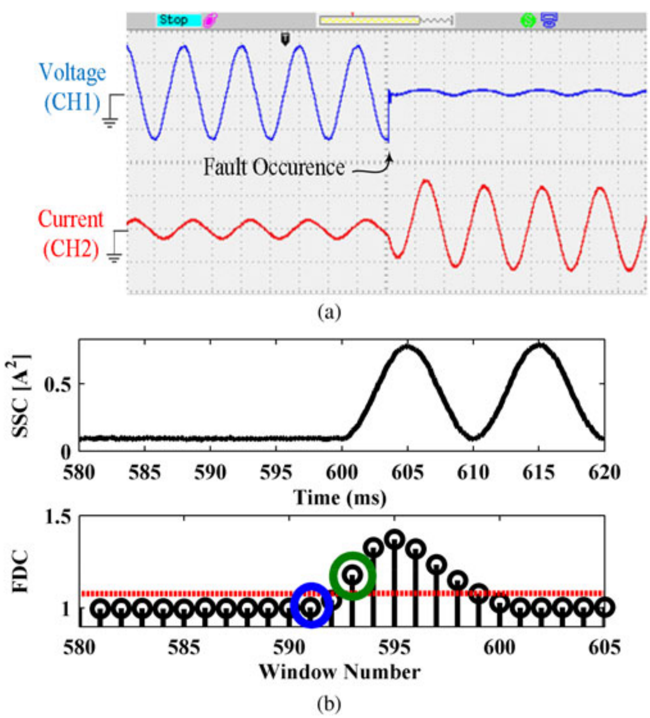

Fig. 14. Evaluation of the method using experimental data. (a) Voltage and current waveforms of the faulty phase during an LG fault in the fourth system. (b) SSC signal and its FDC under this condition.

J. Experimental Data

For final evaluation, the proposed fault detection method is assessed by some gathered experimental data from different experiments carried out on the laboratory system. A typical voltage and current waveforms for an LG fault are shown in Fig. 14(a). In this figure, only the waveforms of faulty phase are displayed. Fig. 14(b) shows the corresponding SSC signal and FDC for this fault. From this figure, it is evident that the proposed method can detect the fault after 2 ms.

K. Sensitivity Analysis

The sensitivity of the proposed algorithm is assessed under different fault conditions including fault types, fault resistances, fault location, and fault inception time. The results are presented

This article has been accepted for inclusion in a future issue of this journal. Content is final as presented, with the exception of pagination.

TABLE III
SENSITIVITY OF THE PROPOSED METHOD TO DIFFERENT FAULT CONDITIONS

CASE	*AVERAGE FAULT DETECTION TIME (MS)*	*THE PROPOSED METHOD PERFORMANCE (%)*
DIFFERENT FAULT TYPES		
LG FAULTS	1.862	99.28
LL FAULTS	1.741	98.12
LLG FAULTS	1.712	99.05
LLL FAULTS	1.769	99.32
DIFFERENT FAULT RESISTANCE		
$0\ \Omega < R_F < 60\ \Omega$	1.718	99.54
$60\ \Omega < R_F < 120\ \Omega$	1.724	99.17
$120\ \Omega < R_F < 180\ \Omega$	1.788	98.91
$180\ \Omega < R_F < 240\ \Omega$	1.806	97.89
DIFFERENT FAULT LOCATION		
$1\ \% < D_F < 25\ \%$	1.709	99.89
$25\ \% < D_F < 50\ \%$	1.715	99.57
$50\ \% < D_F < 75\ \%$	1.766	99.57
$75\ \% < D_F < 99\ \%$	1.802	98.82
DIFFERENT FAULT INCEPTION ANGLE		
$0^0 < T_F < 45^0$	1.724	99.22
$45^0 < T_F < 90^0$	1.718	98.76
$90^0 < T_F < 135^0$	1.779	99.09
$135^0 < T_F < 180^0$	1.731	97.76

in Table III. It should be mentioned that all simulation and experimental data were considered in this analysis. In Table III, R_f denotes the value of fault resistance, D_f denotes the fault location as percentage of TL length, and T_f indicates the angle of fault occurrence. The analysis is performed for a wide range of the mentioned fault conditions.

As observed in Table III, the elapsed time for fault identification dramatically increases in case of LG fault types, fault resistance more than 180 Ω, fault location more than 50% of the TL, and fault inception angle in the range of 90–135°. Also, the accuracy of the method decreases in case of LL fault types, fault resistance more than 180 Ω, fault location more than 75% of the TL, and fault inception angle in the range of 135–180°. It is clear that the proposed method has a sufficiently good performance for all of the fault conditions.

L. Discussion About Window Length and Time Step

The appropriate window length and time step of the proposed method are selected using a trial and error-based approach. In the following, more details regarding these selections are presented.

Different values of window length and time step are considered, and then accuracy and speed of the method are determined for them. These results are tabulated in Table IV. All the scenarios mentioned in last sections are considered for selecting desirable window length and time step. In this table, *accuracy of method* is the average of the accuracy in four described systems. The index *average fault detection time* is the average of the proposed method time delay and index *maximum fault detection time* shows the maximum time delay at which faults can be identified. As shown in Table IV, ten different cases are investigated, in which the window length is considered as constant (window length = 5, 6, 7, 8, 9, 10, 11, 12, 13, and 14 ms) and the value of the time step is varied from 0.5 to 2 ms with the step of 0.5 ms (time step = 0.5, 1, 1.5, and 2 ms). Totally, 40 different scenarios are considered for the window length and time step of the proposed method. Considering the presented results in Table IV, window length and time step are considered 10 ms and 1 ms, respectively, by making a compromise between accuracy and delay of the method.

TABLE IV
RESULTS OF THE METHOD FOR DIFFERENT WINDOW LENGTHS AND TIME STEPS

CASE	*WINDOW LENGTH (MS)*	*TIME STEP (MS)*	*AVERAGE FAULT DETECTION TIME (MS)*	*MAXIMUM FAULT DETECTION TIME (MS)*	*ACCURACY OF PROPOSED METHOD (%)*
1	5	0.5	81.342	1.523	2.5
		1	84.157	1.574	3
		1.5	83.214	1.531	3
		2	86.524	1.615	6
2	6	0.5	88.149	1.596	2.5
		1	84.829	1.557	4
		1.5	88.486	1.621	6
		2	87.653	1.607	6
3	7	0.5	89.369	1.591	2.5
		1	88.343	1.573	3
		1.5	85.641	1.627	6
		2	87.249	1.609	6
4	8	0.5	91.054	1.568	3
		1	90.963	1.574	4
		1.5	89.356	1.616	6
		2	96.746	1.662	4
5	9	0.5	94.678	1.597	4
		1	95.691	1.599	4
		1.5	95.278	1.686	6
		2	97.359	1.672	6
6	10	0.5	97.259	1.676	4
		1	99.175	1.705	4
		1.5	98.741	1.759	6
		2	99.076	1.819	6
7	11	0.5	98.146	1.703	4.5
		1	99.351	1.742	4
		1.5	98.931	1.763	6
		2	99.127	1.803	6
8	12	0.5	98.379	1.798	5
		1	99.023	1.823	5
		1.5	99.258	1.867	6
		2	99.095	1.889	6
9	13	0.5	97.282	1.869	5.5
		1	97.783	1.869	5
		1.5	94.561	1.925	6
		2	97.349	1.989	6
10	14	0.5	96.147	1.869	5
		1	96.915	1.957	5
		1.5	97.022	2.028	6
		2	97.335	2.47	6

TABLE V
DELAY TIME AND PERFORMANCE OF THE PROPOSED METHOD IN THE FOUR SYSTEMS

SYSTEM	*MEAN FAULT DETECTION TIME (MS)*	*PROPOSED METHOD PERFORMANCE (%)*
FIRST SYSTEM	1.65	99
SECOND SYSTEM	1.58	99
THIRD SYSTEM	1.76	98.43
FOURTH SYSTEM	1.83	96.67

M. Summary of the Results

In this section, the gathered results from the four described systems are tabulated in Table V. In this table, the average

This article has been accepted for inclusion in a future issue of this journal. Content is final as presented, with the exception of pagination.

TABLE VI
RESULTS OF COMPARISON WITH SOME OTHER SIMILAR METHODS

METHOD	*ACCURACY IN STUDIED SYSTEM (%)*				*MEAN FAULT DETECTION TIME (MS)*	*MAXIMUM FAULT DETECTION TIME (MS)*	*THRESHOLD VALUE (P.U)*	*COMPUTATIONAL BURDEN*
	FIRST SYSTEM	*SECOND SYSTEM*	*THIRD SYSTEM*	*FOURTH SYSTEM*				
A	46.33	55.3	35.6	67.5	4.08	7.35	10	LOW
B	87.67	76.67	77.5	82.6	4.15	7.48	20	LOW
C	81.67	67.33	79.4	85.5	3.75	6.86	50	LOW
D	87.33	85.6	91.5	87.7	3.88	6.95	25	HIGH
E	95.21	93.37	95.24	94.5	5	5	12	HIGH
F	91.67	90.87	93.5	91.2	2.95	4.71	25	HIGH
G	87.33	88.25	92.45	89.3	3.11	5.12	0.8	LOW
PROPOSED METHOD	**99**	**98.43**	**99**	**96.67**	**1.705**	**4**	**1.1**	**LOW**

time for fault detection and its performance for each system are presented. The average time is calculated by averaging the fault detection time delays for all data of each system under the different conditions. Also, the method performance is calculated by dividing number of algorithm maloperations on all the test cases. From the results, the delay time of the proposed method is about 1.7 ms. Moreover, the proposed method has a desirable accuracy in the different systems.

V. COMPARISON WITH PREVIOUS METHODS

In this section, the performance and accuracy of the proposed method are compared with some other similar approaches. All the methods are evaluated using the same data under similar conditions. The studied methods are briefly reviewed as follows.

1) *Sample-to-sample comparison method [36]:* In this method, the difference between the present and previous samples is calculated and it is compared to a threshold value for detection of the fault. At the steady state of the power system, the difference is expected to be a fixed value, while it increases at faulty conditions, significantly.
2) *Cycle-to-cycle comparison method [36]:* This method is based on the difference of sample values, which has a distance of one cycle. This difference is expected to be zero under the normal condition, whereas it would be high enough after any fault occurrence.
3) *Moving sum method [37]:* This approach is based on the calculation of one cycle summation on current samples for one side of TLs. It is found on symmetrical nature of current waveforms in power systems. Under the normal condition, the summation is near to zero. However, it exceeds a predefined threshold under the fault condition.
4) *Cumulative sum (CUSUM) method [38]:* This method compares values of the samples using a predetermined drift parameter "v," which is equal to the relay setting current. It uses current samples $s(k)$ and defines two complementary signals $s_1(k)$, $s_2(k)$, which are positive and negative parts of $s(k)$. The CUSUM method has two indices $g_k(1)$ and $g_k(2)$ as fault indices during positive and negative cycles, respectively. If either of the indices exceeds the relay setting current, the fault is detected.
5) *Difference in energy of S-transform for current signals [39]:* S-transform has been widely used in fault detection methods because of its superiority in localizing the instant of fault occurrence and simultaneously providing good information about amplitude and phase of voltage and current signals. In this method, current signals are processed through S-transform to generate some certain frequency contours. In next step, the difference in energy of each processed current signal is computed for every half-cycle. If this difference reaches a predefined threshold, the fault is detected.
6) *Discrete wavelet transform of the current signal [40]:* Wavelet transform is an efficient means of analyzing transient currents and voltages in power system protections. In this method, the three-phase currents of TL are analyzed with db 4 mother wavelet to obtain the detail coefficients over a moving window of half-cycle length. Summation of these detail coefficients in the mentioned moving window is compared with a selected threshold. If this index exceeds the threshold, the fault is detected.
7) *Difference in the correlation coefficient of the current signal [41]:* This method is based on correlation coefficients derived by the conventional correlation formula for two half successive cycles of the current signal with the same polarity. This method only needs measurement of three-phase currents. Correlation coefficients magnitude is compared with a predefined threshold to detect fault conditions.

In following, the performance of the proposed technique is compared with the aforementioned methods based on five criteria including accuracy, required average time and maximum time for fault detection, threshold value in per-unit, and computational burden. The total number of these case studies is more than 700. In Table VI, the results are tabulated. It is obvious that the proposed method can successfully detect the faults, while other methods have false operation in some cases. Moreover, the average time delay of the proposed scheme is about 1.7 ms and its maximum fault detection time is 4 ms. Also, the computational burden of the proposed method is considerably low in comparison with the other methods.

VI. CONCLUSION

A simple fault detection algorithm for TLs was proposed. The suggested algorithm is based on the moving average of the SSC

This article has been accepted for inclusion in a future issue of this journal. Content is final as presented, with the exception of pagination.

signal. A new criterion using moving average concept is defined for the detection of different faults. The results confirmed that the proposed method can successfully handle controversial situations such as heavy load switching, fault with high resistances, faults near boundaries, mutual coupling effects, noisy situation, intercircuit faults, power swing circumstances, faults in series-compensated lines, and CT saturation effects. Also, the results approved that the performance of the method is independent of the network structure. It only requires about 1.7 ms for fault identification with a relatively low calculation burden.

References

[1] K. Chen, C. Huang, and J. He, "Fault detection, classification and location for transmission lines and distribution systems: A review on the methods," *High Voltage*, vol. 1, pp. 25–33, 2016.

[2] M. K. Jena, S. R. Samantaray, and B. K. Panigrahi, "A new decentralized approach to wide-area back-up protection of transmission lines," *IEEE Syst. J.*, to be published, doi: 10.1109/JSYST.2017.2694453.

[3] M. Jannati, B. Vahidi, S. H. Hosseinian, and H. R. Baghaee, "A new adaptive single phase auto-reclosure scheme for EHV transmission lines," in *Proc. 12th Int. Middle-East Power Syst. Conf.*, 2008, pp. 203–207.

[4] T. S. Abdelgayed, W. G. Morsi, and T. S. Sidhu, "Fault detection and classification based on co-training of semisupervised machine learning," *IEEE Trans. Ind. Electron.*, vol. 65, no. 2, pp. 1595–1605, Feb. 2018.

[5] M. Jannati, S. Jazebi, B. Vahidi, and S. Hosseinian, "A novel algorithm for fault type fast diagnosis in overhead transmission lines using hidden Markov models," *J. Electr. Eng. Technol.*, vol. 6, pp. 742–749, 2011.

[6] R. Dubey, S. R. Samantaray, B. K. Panigrahi, and V. G. Venkoparao, "Koopman analysis based wide-area back-up protection and faulted line identification for series-compensated power network," *IEEE Syst. J.*, to be published, doi: 10.1109/JSYST.2016.2615898.

[7] P. Kundu and A. K. Pradhan, "Power network protection using wide-area measurements considering uncertainty in data availability," *IEEE Syst. J.*, to be published, doi: 10.1109/JSYST.2017.2721641.

[8] M. A. Jarrahi, H. Samet, and A. Sahebi, "An EMD based fault type identification scheme in transmission line," in *Proc. 24th Iranian Conf. Electr. Eng.*, 2016, pp. 422–427.

[9] J. Moshtagh, M. Jannati, H. Baghaee, and E. Nasr, "A novel approach for online fault detection in HVDC converters," in *Proc. 12th Int. Middle-East Power Syst. Conf.*, 2008, pp. 307–311.

[10] A. A. Majd, H. Samet, and T. Ghanbari, "k-NN based fault detection and classification methods for power transmission systems," *Protection Control Mod. Power Syst.*, vol. 2, 2017, Art. no. 32.

[11] M. Jannati, B. Vahidi, S. H. Hosseinian, and H. R. Baghaee, "A novel approach for optimizing dead time of extra high voltage transmission lines," in *Proc. 11th Int. Conf. Optim. Electr. Electron. Equipment*, 2008, pp. 215–220.

[12] B. Rathore and A. G. Shaik, "Wavelet-alienation based transmission line protection scheme," *IET Gener., Transm. Distrib.*, vol. 11, no. 4, pp. 995–1003, 2017.

[13] S. Samantaray and P. Dash, "Transmission line distance relaying using a variable window short-time Fourier transform," *Electr. Power Syst. Res.*, vol. 78, pp. 595–604, 2008.

[14] G. Ziegler, *Numerical Distance Protection: Principles and Applications*. Hoboken, NJ, USA: Wiley, 2011.

[15] E. Koley, R. Kumar, and S. Ghosh, "Low cost microcontroller based fault detector, classifier, zone identifier and locator for transmission lines using wavelet transform and artificial neural network: A hardware co-simulation approach," *Int. J. Electr. Power Energy Syst.*, vol. 81, pp. 346–360, 2016.

[16] B. Ravikumar, D. Thukaram, and H. Khincha, "Application of support vector machines for fault diagnosis in power transmission system," *IET Gener., Transm. Distrib.*, vol. 2, no. 1, pp. 119–130, 2008.

[17] J. Upendar, C. Gupta, and G. Singh, "Statistical decision-tree based fault classification scheme for protection of power transmission lines," *Int. J. Electr. Power Energy Syst.*, vol. 36, pp. 1–12, 2012.

[18] F. Costa, A. Monti, F. Lopes, K. Silva, P. Jamborsalamati, and A. Sadu, "Two-terminal traveling-wave-based transmission-line protection," *IEEE Trans. Power Del.*, vol. 32, no. 3, pp. 1382–1393, Jun. 2017.

[19] S. Hasheminejad, S. G. Seifossadat, M. Razaz, and M. Joorabian, "Ultra-high-speed protection of transmission lines using traveling wave theory," *Electr. Power Syst. Res.*, vol. 132, pp. 94–103, 2016.

[20] X.-N. Lin, M. Zhao, K. Alymann, and P. Liu, "Novel design of a fast phase selector using correlation analysis," *IEEE Trans. Power Del.*, vol. 20, no. 2, pp. 1283–1290, Apr. 2005.

[21] R. Mahanty and P. D. Gupta, "A fuzzy logic based fault classification approach using current samples only," *Electr. Power Syst. Res.*, vol. 77, pp. 501–507, 2007.

[22] A. Rahmati and R. Adhami, "A fault detection and classification technique based on sequential components," *IEEE Trans. Ind. Appl.*, vol. 50, no. 6, pp. 4202–4209, Nov./Dec. 2014.

[23] S. H. Horowitz and A. G. Phadke, *Power System Relaying*, vol. 22. Hoboken, NJ, USA: Wiley, 2008.

[24] J. G. Rao and A. K. Pradhan, "Power-swing detection using moving window averaging of current signals," *IEEE Trans. Power Del.*, vol. 30, no. 1, pp. 368–376, Feb. 2015.

[25] N. Otsu, "A threshold selection method from gray-level histograms," *IEEE Trans. Syst., Man, Cybern.*, vol. SMC-9, no. 1, pp. 62–66, Jan. 1979.

[26] E. Cuevas and H. Sossa, "A comparison of nature inspired algorithms for multi-threshold image segmentation," *Expert Syst. Appl.*, vol. 40, pp. 1213–1219, 2013.

[27] H. Samet, A. Shabanpour-Haghighi, and T. Ghanbari, "A fault classification technique for transmission lines using an improved alienation coefficients technique," *Int. Trans. Electr. Energy Syst.*, vol. 27, 2016, Art. no. e2235.

[28] M. A. Jarrahi, H. Samet, H. Raayatpisheh, A. Jafari, and M. Rakhshan, "An ANFIS-based fault classification approach in double-circuit transmission line using current samples," in *Proc. Int. Work-Conf. Artif. Neural Netw.*, 2015, pp. 225–236.

[29] P. W. Sauer and M. Pai, *Power System Dynamics and Stability*. Upper Saddle River, NJ, USA: Prentice-Hall, 1998.

[30] A. Yadav and A. Swetapadma, "A finite-state machine based approach for fault detection and classification in transmission lines," *Electr. Power Compon. Syst.*, vol. 44, pp. 43–59, 2016.

[31] A. Yadav and A. Swetapadma, "Enhancing the performance of transmission line directional relaying, fault classification and fault location schemes using fuzzy inference system," *IET Gener., Transm. Distrib.*, vol. 9, no. 6, pp. 580–591, 2015.

[32] A. Swetapadma and A. Yadav, "Data-mining-based fault during power swing identification in power transmission system," *IET Sci., Meas. Technol.*, vol. 10, pp. 130–139, 2016.

[33] V. H. Makwana and B. Bhalja, "New adaptive digital distance relaying scheme for double infeed parallel transmission line during inter-circuit faults," *IET Gener., Transm. Distrib.*, vol. 5, no. 6, pp. 667–673, Jun. 2011.

[34] M. K. Jena, S. Samantaray, and B. K. Panigrahi, "A new wide-area backup protection scheme for series-compensated transmission system," *IEEE Syst. J.*, vol. 11, no. 3, pp. 1877–1887, Sep. 2017.

[35] M. L. S. Almeida and K. M. Silva, "Transmission lines differential protection based on an alternative incremental complex power alpha plane," *IET Gener., Transm. Distrib.*, vol. 11, no. 1, pp. 10–17, 2017.

[36] A. G. Phadke and J. S. Thorp, *Computer Relaying for Power Systems*. Hoboken, NJ, USA: Wiley, 2009.

[37] A. Pradhan, A. Routray, and S. Mohanty, "A moving sum approach for fault detection of power systems," *Electr. Power Compon. Syst.*, vol. 34, pp. 385–399, 2006.

[38] S. Mohanty, A. Pradhan, and A. Routray, "A cumulative sum-based fault detector for power system relaying application," *IEEE Trans. Power Del.*, vol. 23, no. 1, pp. 79–86, Jan. 2008.

[39] P. K. Dash, S. Das, and J. Moirangthem, "Distance protection of shunt compensated transmission line using a sparse S-transform," *IET Gener., Transm. Distrib.*, vol. 9, no. 12, pp. 1264–1274, 2015.

[40] A. R. Adly, R. A. El Sehiemy, and A. Y. Abdelaziz, "A novel single end measuring system based fast identification scheme for transmission line faults," *Measurement*, vol. 103, pp. 263–274, 2017.

[41] M. Eissa and M. Mahfouz, "New high-voltage directional and phase selection protection technique based on real power system data," *IET Gener., Transm. Distrib.*, vol. 6, no. 11, pp. 1075–1085, 2012.

Authors' photographs and biographies not available at the time of publication.